NASA/TM—2012-217252 AIAA–2011–2912

Full-Scale Turbofan-Engine Turbine-Transfer Function Determination Using Three Internal Sensors

Lennart S. Hultgren
Glenn Research Center, Cleveland, Ohio

February 2012

NASA STI Program . . . in Profile

Since its founding, NASA has been dedicated to the advancement of aeronautics and space science. The NASA Scientific and Technical Information (STI) program plays a key part in helping NASA maintain this important role.

The NASA STI Program operates under the auspices of the Agency Chief Information Officer. It collects, organizes, provides for archiving, and disseminates NASA's STI. The NASA STI program provides access to the NASA Aeronautics and Space Database and its public interface, the NASA Technical Reports Server, thus providing one of the largest collections of aeronautical and space science STI in the world. Results are published in both non-NASA channels and by NASA in the NASA STI Report Series, which includes the following report types:

- TECHNICAL PUBLICATION. Reports of completed research or a major significant phase of research that present the results of NASA programs and include extensive data or theoretical analysis. Includes compilations of significant scientific and technical data and information deemed to be of continuing reference value. NASA counterpart of peer-reviewed formal professional papers but has less stringent limitations on manuscript length and extent of graphic presentations.

- TECHNICAL MEMORANDUM. Scientific and technical findings that are preliminary or of specialized interest, e.g., quick release reports, working papers, and bibliographies that contain minimal annotation. Does not contain extensive analysis.

- CONTRACTOR REPORT. Scientific and technical findings by NASA-sponsored contractors and grantees.

- CONFERENCE PUBLICATION. Collected papers from scientific and technical conferences, symposia, seminars, or other meetings sponsored or cosponsored by NASA.

- SPECIAL PUBLICATION. Scientific, technical, or historical information from NASA programs, projects, and missions, often concerned with subjects having substantial public interest.

- TECHNICAL TRANSLATION. English-language translations of foreign scientific and technical material pertinent to NASA's mission.

Specialized services also include creating custom thesauri, building customized databases, organizing and publishing research results.

For more information about the NASA STI program, see the following:

- Access the NASA STI program home page at *http://www.sti.nasa.gov*

- E-mail your question via the Internet to *help@sti.nasa.gov*

- Fax your question to the NASA STI Help Desk at 443–757–5803

- Telephone the NASA STI Help Desk at 443–757–5802

- Write to:
  NASA Center for AeroSpace Information (CASI)
  7115 Standard Drive
  Hanover, MD 21076–1320

NASA/TM—2012-217252 AIAA–2011–2912

Full-Scale Turbofan-Engine Turbine-Transfer Function Determination Using Three Internal Sensors

Lennart S. Hultgren
Glenn Research Center, Cleveland, Ohio

Prepared for the
17th Aeroacoustics Conference
cosponsored by the American Institute of Aeronautics and Astronautics and
the Confederation of European Aerospace Societies
Portland, Oregon, June 5–8, 2011

National Aeronautics and
Space Administration

Glenn Research Center
Cleveland, Ohio 44135

February 2012

Acknowledgments

This work was supported by the NASA Fundamental Aeronautics Program Subsonic Fixed Wing Project (SFW). The NASA Fundamental Aeronautics Program has the principal objective of overcoming today's national challenges in air transportation. The work herein is aligned with the SFW Reduce-Perceived-Noise Technical Challenge, which aims to enable concepts and technologies to dramatically reduce the perceived aircraft noise outside of airport boundaries. It is part of a NASA-internal and NASA-sponsored external research effort for the development and improvement of aircraft noise-prediction capability and tools.

Trade names and trademarks are used in this report for identification only. Their usage does not constitute an official endorsement, either expressed or implied, by the National Aeronautics and Space Administration.

This work was sponsored by the Fundamental Aeronautics Program at the NASA Glenn Research Center.

Level of Review: This material has been technically reviewed by technical management.

Available from

NASA Center for Aerospace Information
7115 Standard Drive
Hanover, MD 21076–1320

National Technical Information Service
5301 Shawnee Road
Alexandria, VA 22312

Available electronically at http://www.sti.nasa.gov

Full-Scale Turbofan-Engine Turbine-Transfer Function Determination Using Three Internal Sensors

Lennart S. Hultgren
National Aeronautics and Space Administration
John H. Glenn Research Center at Lewis Field
Cleveland, Ohio 44135, USA

Noise-source separation techniques, using three engine-internal sensors, are applied to existing static-engine test data to determine the turbine transfer function for the currently sub-dominant combustion noise. The results are used to assess the combustion-noise prediction capability of the Aircraft Noise Prediction Program (ANOPP) and an improvement to the combustion-noise module GECOR is suggested. The work was carried out in response to the NASA Fundamental Aeronautics Subsonic Fixed Wing Program's Reduced-Perceived-Noise Technical Challenge.

I. Introduction

The reduction of aircraft noise is critical for enabling the anticipated large increase in future air traffic. Noise generated in the jet engine core, by components such as the compressor, combustor, and turbine, can be significant contributors to the overall noise signature at low-power conditions, typical of approach flight. At high engine power settings during takeoff, jet and fan noise have traditionally dominated over core noise for existing engines. However, current design trends and expected technological advances in engine-cycle design as well as noise-reduction methods are likely to reduce non-core-noise contributions even at engine-power points higher than approach. The result of such changes will be to elevate the overall importance of core noise. New airport regulations are likely to require additional noise reductions, thus emphasizing the need for further reductions in core noise.

The present paper is concerned with the combustion noise component of the core noise. The unsteady combustion process is the source of pressure, entropy, and vorticity fluctuations. The noise frequency is set by the unsteady combustion process and its peak value is generally believed to fall in the range of 400–500 Hz. Combustion noise is of either the direct or indirect type. A fraction of the pressure disturbances are acoustic pressure fluctuations with the balance being hydrodynamical unsteadiness. The former is what is referred to as direct combustion noise. Its spectrum is modified by the combustor geometry as well as pressure feedback on the unsteady combustion process itself. The direct combustion noise is reduced due to transmission effects during its propagation through the turbine stages. The combustor entropy (temperature) fluctuations are convected downstream with the local mean velocity and get converted to acoustic pressure fluctuations in the turbine and other regions of rapid flow change. This is the indirect process of turbomachinery combustion noise generation. This is potentially a very effective mechanism and occurs at all turbine stages. The indirect noise occurs in the same basic frequency range as the direct noise, but their spectral-distribution shapes could be quite different. Figure 1 illustrates the dual paths of combustion noise. Note that the direct and indirect noise contributions are correlated at the source because both are caused by the unsteady heat addition. The relative importance of direct and indirect combustion noise contributions is still an unresolved issue.[1–6]

Direct measurement of turbofan-engine combustion noise is difficult because of the presence of jet noise in the frequency range of interest. Since flight effects reduce jet noise more than combustion noise, combustion noise can be a significant contributor to aircraft approach noise but may be masked by jet noise under the corresponding static-engine test condition. To overcome this obstacle, researchers[7–19] developed coherence techniques utilizing engine-internal as well as far-field measurements to identify the far-field combustion noise component. Modal analyses[20–24] were also carried out to determine the source and propagation characteristics of combustion noise.

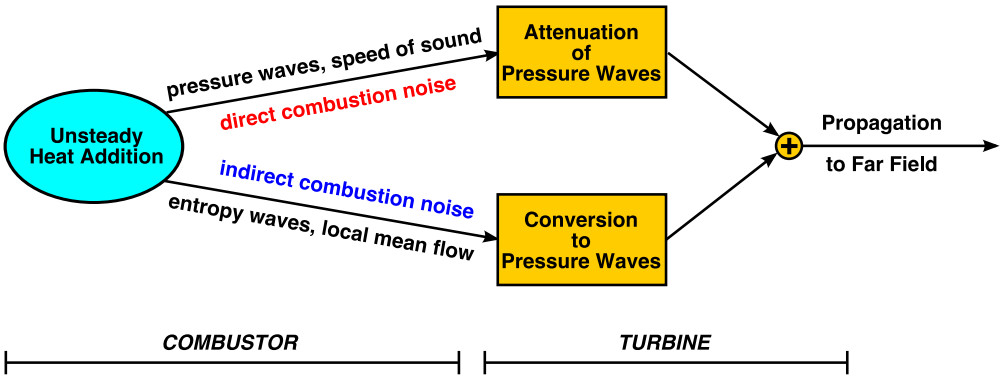

Figure 1. Dual paths for combustion noise

Hultgren and Miles[25] discussed noise-source separation techniques for application to engine test-stand data and assessed a current prediction method[26,27] applied to a static-engine test.[28] The current paper is an extension of this work in that a determination of the turbine transfer function is attempted.

II. Data Analysis

A. Static-Engine Test Data

Data obtained from the NASA/Honeywell Engine Validation of Noise and Emission Reduction Technology program[28] (EVNERT) is used herein to assess the turbine transfer of direct combustion-noise and the creation of indirect combustion noise through entropy/blade-row interactions in the turbine. This static engine test activity was carried out in Honeywell Aerospace's San Tan outdoor test facility from 2005 to 2007. The program used the Honeywell TECH977 research engine, which is typical of a business-jet application in the 6,000–8,000 lbs thrust class.

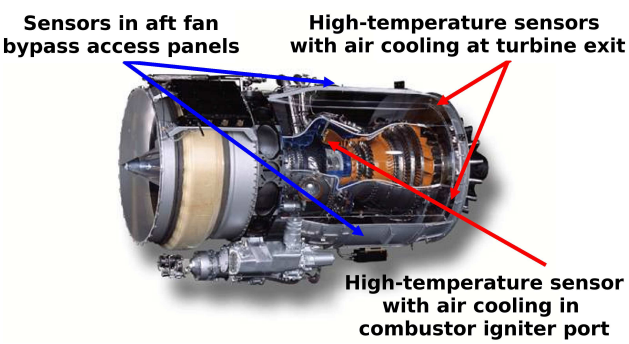

Figure 2. Honeywell TECH977 turbofan engine-internal sensors

The engine-internal instrumentation in EVNERT configuration 35 included high-temperature pressure sensors with air cooling in a combustor ingnitor port (CIP1) and at the turbine exit (T551 and T552). Pressure time histories at the internal sensors CIP1, T551, and T552 herein. The EVNERT data acquisition system had a sampling rate of 65,536 Hz and a duration of about 70 s, leading to time histories with just over 4.5 million data points. Each time series is analyzed here using an FFT length of 8192 points (corresponding to an 8 Hz frequency resolution or bin width), Hanning windowing, and a 50 percent data-segment overlap. The narrowband auto spectra, resulting from $M = 1117$ averages, then can be summed up to yield the corresponding 1/3-octave sound-pressure level (SPL). The 130° 1/3-octave far-field total SPL result was found to be in full agreement with the Honeywell provided 1/3-octave SPL data.[25]

Royalty and Schuster[24] analyzed the acoustic modes in the combustor for a different arrangement of the EVNERT turbofan engine than considered herein. In that configuration,[28] the fan was replaced by a water brake in order to remove fan sources from the total noise signature. The no-fan configuration could be operated up to a power setting corresponding to the approach condition of 60 % corrected fan speed. The combustor internal instrumentation consisted of a circumferential array of 16 equally-spaced pressure probes. They[24] (see their Fig. 19) found that for low frequencies most of the acoustic energy was associated with the plane wave ($m = 0$) mode, that the first circumferential mode ($m = \pm 1$) was dominant in the frequency range of 500–1000 Hz, and that higher circumferential modes ($m = \pm 2$, $m = \pm 3$, $m = \pm 3, \ldots$) sequentially became the most significant feature at successively higher frequencies, where m is the azimuthal wave number or mode order. One can observe in their figure that at 500 Hz, the plane wave mode is about 8 dB and 5 dB below the total acoustic level at the 48 % and 60 % power settings, respectively. They also reported that the higher modes ($m \neq 0$) were not present in the far-field data. It is concluded here that this indicates

that the non-plane-wave modes are cut-off in the turbine/duct downstream of the combustor for this particular engine. This is in agreement with the results of Hultgren and Miles[25] in which coherent combustion noise was only found for frequencies less than about 400+ Hz.

B. Frequency Response Functions

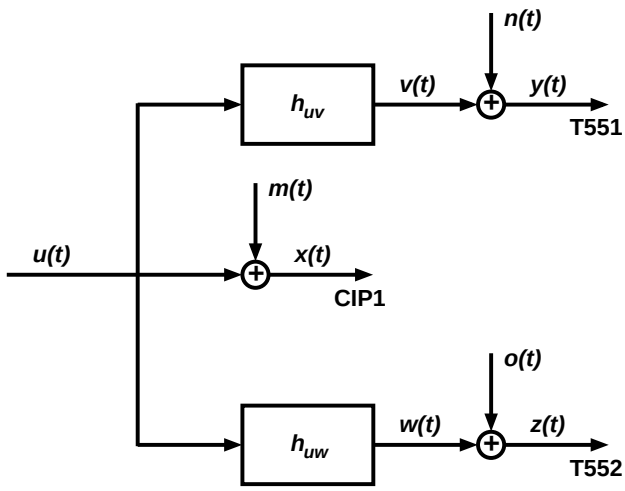

Figure 3. Schematic Diagram for Coherence-Technique Measurements

Figure 3 illustrates the relationships between the signals measured by the engine-internal sensors CIP1, T551, and T552. The signals $u(t)$, $v(t)$, and $w(t)$ represent the coherent acoustic combustion-noise signal at the three sensors as functions of time t. These 'desired' signals cannot be directly obtained by themselves because of the presence of the random uncorrelated 'noise' signals $m(t)$, $n(t)$, and $o(t)$ at the different measuring stations. However, the downstream signals $v(t)$ and $w(t)$ are uniquely determined by the previous-station signal $u(t)$ and the impulse-response functions h_{uv} and h_{uw}, respectively. The measurable signal, $x(t)$, $y(t)$, or $z(t)$, at each sensor is the sum of the 'desired' and corresponding 'noise' signals. The signals $m(t)$, $n(t)$, and $o(t)$ can be taken as mutually uncorrelated as well as uncorrelated with the combustion-noise signal $u(t)$, $v(t)$, or $w(t)$ at all the stations. The signal $m(t)$ is to a large extent caused by hydrodynamical pressure fluctuations (pseudo sound) in the combustor and possibly also higher acoustic modes present in the combustor but cut-off in the downstream tail pipe and can potentially be quite large. The signals $n(t)$ and $o(t)$ are mainly due to acoustic pressure fluctuations from other noise sources and can actually be correlated if turbine broadband noise is also present at the frequencies of interest.

The goal of the present work is to determine the frequency response functions

$$H_{uv}(f) \equiv G_{uv}(f)/G_{uu}(f) = G_{xy}(f)/G_{uu}(f) = H_{xy}(f)[1 + N_u(f)]\,, \tag{1a}$$

$$H_{uw}(f) \equiv G_{uw}(f)/G_{uu}(f) = G_{xz}(f)/G_{uu}(f) = H_{xz}(f)[1 + N_u(f)]\,, \tag{1b}$$

$$H_{vw}(f) \equiv G_{vw}(f)/G_{vv}(f) = [1 - \delta(f)]G_{yz}(f)/G_{vv}(f)\,, \tag{1c}$$

$$H_{wv}(f) \equiv G_{wv}(f)/G_{ww}(f) = [1 - \delta^*(f)]G^*_{yz}(f)/G_{ww}(f)\,, \tag{1d}$$

where f is the frequency and the star denotes complex conjugation. $G_{\alpha\alpha}$ and $G_{\alpha\beta}$ denote the one-sided auto-spectrum and cross-spectrum of the signals α and β, where α and β are dummy indexes. The one-sided auto-spectra $G_{uu}(f)$, $G_{vv}(f)$, and $G_{ww}(f)$ represent the combustion-noise component of the total noise signature $G_{xx}(f)$, $G_{yy}(f)$, and $G_{zz}(f)$ at each of the measuring stations. $H_{xy}(f) \equiv G_{xy}(f)/G_{xx}(f)$ and $H_{xz}(f) \equiv G_{xz}(f)/G_{xx}(f)$ can be thought of as 'directly measured' frequency transfer functions;

$$N_u(f) = G_{mm}(f)/G_{uu}(f) \tag{2}$$

is a real and positive quantity representing the noise to signal ratio at the originating measuring station and is not directly obtainable; and

$$\delta(f) = G_{no}(f)/G_{yz}(f) \tag{3}$$

is a measure of the relative strength of the possible correlation between the $n(t)$ and $o(t)$ signals. $\delta(f)$ describes the influence of broadband turbine noise on the results and is assumed to be small in the frequency range of interest here. The frequency response functions are commonly expressed as $H_{\alpha\beta} = |H_{\alpha\beta}|\exp(\mathrm{i}\phi_{\alpha\beta})$, where $|H_{\alpha\beta}|$ and $\phi_{\alpha\beta} = \arg H_{\alpha\beta}$ are referred to as the gain and phase factors, respectively.

Consequently, the 'true' turbine gain factor is always underpredicted by the 'directly measured' one, i.e., $|H_{uv}(f)| \geqslant |H_{xy}(f)|$ and $|H_{uw}(f)| \geqslant |H_{xz}(f)|$. The 'true' turbine phase factors, however, are identical to the 'directly measured' ones since both are obtainable from the same cross-spectrum, i.e, $\phi_{uv}(f) = \phi_{xy}(f) = \arg G_{xy}(f)$ and $\phi_{uw}(f) = \phi_{xz}(f) = \arg G_{xz}(f)$.

To obtain a better estimate for the 'true' frequency response functions than given by (1a) and (1b), with N_u neglected, the one-sided auto-spectra $G_{uu}(f)$, $G_{vv}(f)$, and $G_{ww}(f)$, i.e., the coherent combustion-noise at each of the measuring stations, need to be determined and this is discussed in the next two subsections. The first of the two deals with a two-signal diagnostic technique, commonly referred to as the coherent-output-power method. The next one addresses a three-signal technique.

C. Coherent-Output-Power Method

The basic formulation for the coherent-output-power method is described in the textbook by Bendat and Piersol.[7] If the sensor inside the combustor and the appropriate turbine-exit sensor (Fig. 3) are used in this technique, it follows that the coherent combustion-noise spectrum at the turbine-exit locations are given by

$$G_{vv}(f) = \frac{|G_{uv}(f)|^2}{G_{uu}(f)} = \frac{|G_{xy}(f)|^2}{G_{uu}(f)} = \gamma_{xy}^2(f) G_{yy}(f)[1 + N_u(f)] \tag{4a}$$

$$G_{ww}(f) = \frac{|G_{uw}(f)|^2}{G_{uu}(f)} = \frac{|G_{xz}(f)|^2}{G_{uu}(f)} = \gamma_{xz}^2(f) G_{zz}(f)[1 + N_u(f)] \tag{4b}$$

regardless of the output noise $G_{nn}(f)$ or $G_{oo}(f)$. $\gamma_{\alpha\beta} = |G_{\alpha\beta}|/\sqrt{G_{\alpha\alpha}G_{\beta\beta}}$ is the coherence.

Note that ignoring N_u in (4) is equivalent to replacing G_{uu} with the measured G_{xx}. The latter is a positive-biased estimate for the unknown input spectra G_{uu}. In view of the certain presence of nonpropagating pressure fluctuations in the combustor, i.e., $G_{mm} \neq 0$, ignoring N_u in (4) is quite likely to underpredict the actual coherent output spectrum. Eqs. (1a), (1b) and (4), all with $N_u = 0$, will be referred to as the two-signal method results in what follows.

D. Three-Signal-Coherence Method

Chung[12] developed a three-signal coherence technique for microphone flow-noise rejection. This three-signal method also applies to the situation shown in Fig. 3. The coherent auto-spectra at the three sensors, CIP1, T551, and T552, are, hence, given by[25]

$$|1 - \delta(f)| G_{uu}(f) = \frac{|G_{xy}(f)||G_{xz}(f)|}{|G_{yz}(f)|} = \frac{\gamma_{xy}(f)\gamma_{xz}(f)}{\gamma_{yz}(f)} G_{xx}(f)\,, \tag{5a}$$

$$\frac{G_{vv}(f)}{|1 - \delta(f)|} = \frac{|G_{xy}(f)||G_{yz}(f)|}{|G_{xz}(f)|} = \frac{\gamma_{xy}(f)\gamma_{yz}(f)}{\gamma_{xz}(f)} G_{yy}(f)\,, \tag{5b}$$

$$\frac{G_{ww}(f)}{|1 - \delta(f)|} = \frac{|G_{xz}(f)||G_{yz}(f)|}{|G_{xy}(f)|} = \frac{\gamma_{xz}(f)\gamma_{yz}(f)}{\gamma_{xy}(f)} G_{zz}(f)\,, \tag{5c}$$

where the δ, defined by Eq. (3), reflects the effect of a possible correlation between the $n(t)$ and $o(t)$ signals. The inclusion of the $|1 - \delta|$ factor is a new result. The standard three-signal method is obtained for $\delta = 0$.

The strength of the standard three-signal method is that it involves only measured cross-spectra. The measured cross-spectra are affected by extraneous noise only if this noise correlates between measurement locations. This can often be avoided by an appropriate spatial separation of the sensors involved and the three-signal method then provides unbiased estimates of the coherent auto-spectra. In contrast, measured auto-spectra will always include a positive definite contribution from the extraneous noise.

Krejsa[15] considered the situation consisting of two engine-internal sensors—signals $x(t)$ and $y(t)$—and a far-field microphone—signal $z(t)$—and obtained (5c), with $\delta = 0$, as his far-field result. The three-signal coherence technique used by Krejsa[15,16,18] eliminated the bias error in the coherent combustion-noise measurements due to engine-internal nonpropagating pressure fluctuations. It is also possible to separate core noise from jet noise using three far-field microphones since each would pick up correlated core noise and uncorrelated external noise from the jet.[17,29] As long as the spatial (polar angle) separation of the microphones is large enough, the jet noise at each location can be assumed to be mutually uncorrelated and Eq. (5), with $\delta = 0$, would apply. Mendoza *et al.*[29] analyzed data from the same Honeywell TECH977 static test,[28] as considered herein, using a three-signal far-field method, among other multiple-microphone signal-processing techniques.[19] They found that the method worked well in frequency regions where a single engine-internal source was dominant. The method did not perform well for frequencies for which multiple self-correlated internal noise sources were of comparable magnitude, e.g. in the relatively limited frequency range where combustion noise and turbine-broadband noise overlapped.

Combining the results (5) with the ones in (1) shows that the frequency response functions are given by

$$H_{uv}(f) = |1-\delta(f)|\frac{|G_{yz}(f)|}{|G_{xz}(f)|}\exp[\mathrm{i}\phi_{xy}(f)]\,, \tag{6a}$$

$$H_{uw}(f) = |1-\delta(f)|\frac{|G_{yz}(f)|}{|G_{xy}(f)|}\exp[\mathrm{i}\phi_{xz}(f)]\,, \tag{6b}$$

$$H_{vw}(f) = \frac{|G_{xz}(f)|}{|G_{xy}(f)|}\exp\left(\mathrm{i}\{\phi_{yz}(f)+\arg[1-\delta(f)]\}\right)\,, \tag{6c}$$

$$H_{wv}(f) = \frac{|G_{xy}(f)|}{|G_{xz}(f)|}\exp\left(-\mathrm{i}\{\phi_{yz}(f)+\arg[1-\delta(f)]\}\right) = \frac{1}{H_{vw}(f)}\,. \tag{6d}$$

Eq. (6) with $\delta = 0$ will be referred to as the three-signal results henceforth. In general, δ is a complex quantity, although assumed small here. Consequently, there can be an error in the gain factor for the turbine transfer of combustion noise by using $\delta = 0$ above, due to the actual presence of broadband turbine noise at the same frequency, but the corresponding phase factor will be unaffected. For the turbine-internal transfer functions, the situation is the opposite.

E. Implementation

From a purely theoretical point of view, $0 \leqslant \gamma_{\alpha\beta} \leqslant 1$, with $\gamma_{\alpha\beta} = 0$ meaning that the two signals $\alpha(t)$ and $\beta(t)$ are completely uncorrelated and $\gamma_{\alpha\beta} = 1$ indicating perfectly correlated signals. In practice, only estimates $\hat{\gamma}_{\alpha\beta}$ of the coherence can be obtained using finite data series. The estimated coherence will, in fact, be nonzero even for completely uncorrelated signals,[30,31] i.e., only the interval

$$\epsilon < \hat{\gamma}_{\alpha\beta} \leqslant 1 \tag{7}$$

is meaningful, where

$$\epsilon^2 = 1-(1-P_I)^{1/(N_s-1)} \tag{8}$$

is the P_I-percent confidence interval if the true $\gamma^2_{\alpha\beta}$ is zero and N_s is the number of independent data segments used in obtaining $\hat{\gamma}^2_{\alpha\beta}$. Welch[32] showed, in the context of estimating auto power spectra, that N_s can be replaced by $9M/11$, where M is the number of 50-percent-overlapped segments used in the analysis. Miles[31] suggested that a better estimate for the coherence threshold value, or noise floor, ϵ can be obtained by purposely unaligning the two time series. That is, a time delay is deliberately introduced to ensure that the two resulting finite time series are uncorrelated. The estimated unaligned coherence does not depend on any particular assumptions about the underlying statistical properties of the time series and accounts for any data-segment overlap and algorithms used in the analysis. The unaligned result captures the coherence of any discrete tones present in the signals and also provides an estimate of the minimum observable broadband coherence. Miles[5,31] found that Eq. (8) with $N_s = M$ provided a good estimate of the noise floor. Following Miles,[5,31] the estimated coherence threshold for the present study is $\epsilon = 0.0518$. If the estimated coherence exceeds the threshold the two time series are coupled. If it is less than the threshold the signals are random and appear independent for that particular number of samples/segments.

In the two-signal (coherent-output-power) method calculations carried out here, the estimated coherence $\hat{\gamma}_{\alpha\beta}(f)$ is replaced by the threshold value ϵ if it falls below that value for a particular narrow-band frequency. That is, the estimated narrow-band combustion-noise component, say $\hat{G}_{ww}(f)$, is simply set to $\epsilon^2\hat{G}_{zz}(f)$ for the frequency in question. Otherwise it is given by (4) with $N_u = 0$.

Mathematically, it follows from Eq. (7) that

$$\epsilon^2 < \hat{\gamma}_{xz}\hat{\gamma}_{yz}/\hat{\gamma}_{xy} < \epsilon^{-1}\,. \tag{9}$$

The upper limit of this inequality is an unphysical result in view of Eq. (5) and the fact that $\hat{G}_{ww}$ cannot be larger than $\hat{G}_{zz}$. Clearly, an additional discriminator is needed to ensure a physically realistic three-signal combustion-noise estimate. This is provided by the following necessary condition[25] for Eq. (5) to be valid:

$$\Theta \equiv \arg[G_{xz}\mathrm{conj(G_{yz})}/G_{xy}] = 0\,. \tag{10}$$

The standard deviation (in radians) of the estimate for the cross-spectrum phase angle $\theta_{\alpha\beta} = \arg(G_{\alpha\beta})$ is given by[5,7]

$$\sigma_{\alpha\beta} = \sin^{-1}\sqrt{(1-\gamma^2_{\alpha\beta})/2\gamma^2_{\alpha\beta}N_s}\,. \tag{11}$$

Note that the standard deviation is zero for perfectly correlated signals and increases as the coherence is diminished. Consequently, in the three-signal method calculations carried out here, the estimated narrow-band combustion-noise component for a particular narrow-band frequency, say $\hat{G}_{ww}(f)$, is set to $\epsilon^2\hat{G}_{zz}(f)$ if, any of the estimated coherence values, $\hat{\gamma}_{xz}$, $\hat{\gamma}_{yz}$, or $\hat{\gamma}_{xy}$, fall below the threshold value ϵ, or if the estimated phase angle $\hat{\Theta} > \hat{\sigma}_{xz} + \hat{\sigma}_{yz} + \hat{\sigma}_{xy}$, where $\hat{\sigma}_{\alpha\beta} = \sin^{-1}\sqrt{[1/\max(\hat{\gamma}^2_{\alpha\beta}, \epsilon^2) - 1]/2N_s}$; otherwise it is given by (5).

III. Results

A. Turbine Auto Spectra

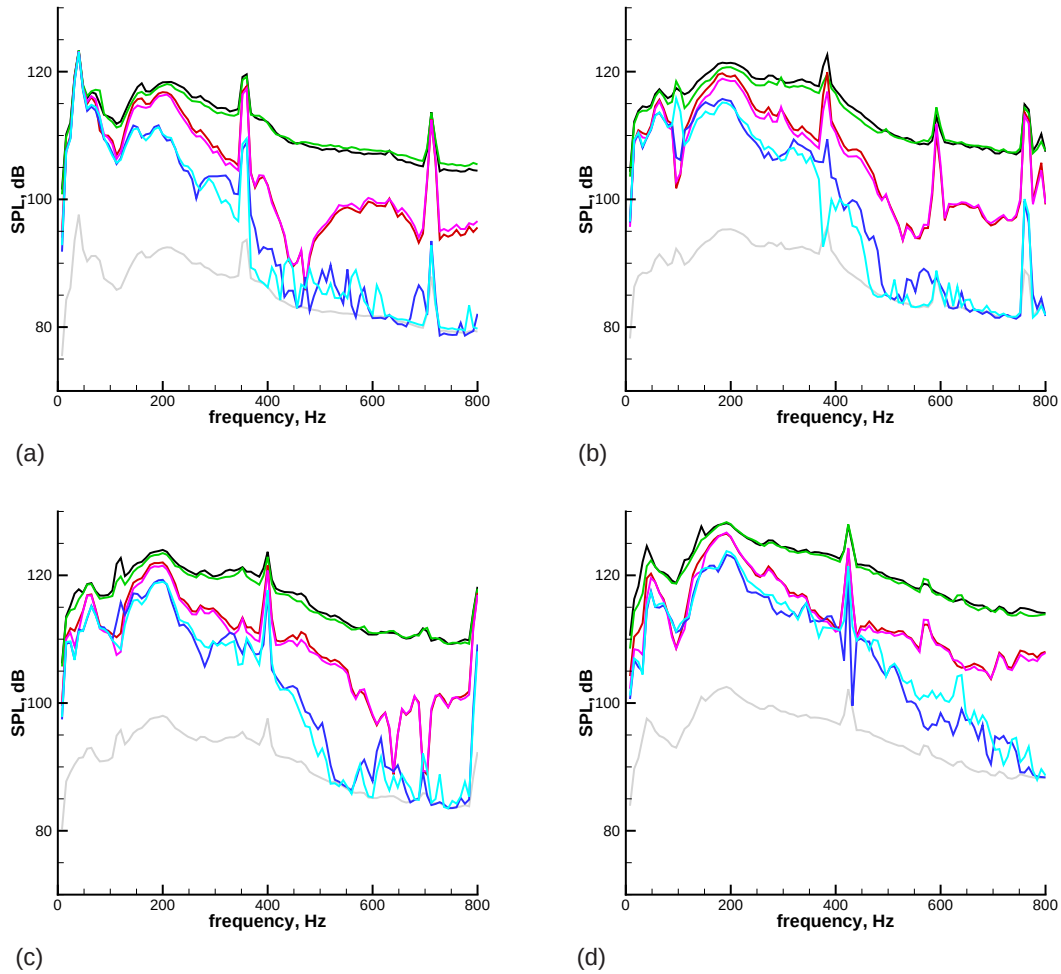

Figure 4. Narrow-band (8 Hz) turbine-internal SPL; black and green curves—total noise signature, G_{yy} and G_{zz}; red and magenta curves—coherent noise using turbine-internal two-signal method, $G_{vv}^{(yz)}$ and $G_{ww}^{(yz)}$; blue and cyan curves—coherent noise using combustor-turbine two-signal method, $G_{vv}^{(xy)}$ and $G_{ww}^{(xz)}$; gray curve—coherence limit, $NOP = \frac{1}{2}\epsilon^2(G_{yy} + G_{zz})$; (a): 48 % corrected fan speed (flight idle); (b): 60 % corrected fan speed (approach); (c): 71 % corrected fan speed (cutback); (d): 87 % corrected fan speed (takeoff)

Figure 4 shows the narrow-band (8 Hz) SPL results, obtained by using two-signal source-separation techniques, at the turbine-exit locations corresponding to the T551 and T552 sensors for the flight-idle, approach, cutback, and takeoff conditions (48, 60, 71, and 87 percent corrected-fan-speed engine power settings) in panels (a) – (d). The black and green curves show the total noise signatures G_{yy} (T551) and G_{zz} (T552), respectively; see Fig. 3 for the signal-sensor labeling scheme. The gray curve shows the average threshold value for the coherent output power, or noise floor, $NOP = \epsilon^2(G_{yy} + G_{zz})/2$. The red and magenta curves show the coherent noise, $G_{vv}^{(yz)} = \gamma^2_{yz}G_{yy}$ and

$G_{ww}^{(yz)} = \gamma_{yz}^2 G_{zz}$, educed by using the signals y and z. These two curves illustrate the coherence between the turbine-exit-sensor signals. The blue and cyan curves show the coherent noise, $G_{vv}^{(xy)} = \gamma_{xy}^2 G_{yy}$ and $G_{ww}^{(xz)} = \gamma_{xz}^2 G_{zz}$, extracted by using the signal pairs (x, y) and (x, z). These latter two curves illustrate the coherence between the signals measured by the combustor sensor (CIP1) and each of the turbine-exit sensors. Allowing for the positive-bias error inherent in two-signal methods, Fig. 4 indicates that the turbine-internal and combustor-turbine methods both yield similar results up to a frequency of about 450 Hz. The increase in coherence seen in the turbine-internal two-signal method curves (red and magenta) occuring at higher frequencies could be an indication of the presence of turbine-broadband noise. However, the deviation between the source-separation results at those frequencies could also be a consequence of an increased bias error in the combustor-turbine method. The former is the more likely scenario, and, in agreement with the results of Hultgren and Miles,[25] it is concluded that coherent combustion noise is present for frequencies up to about 450 Hz at the turbine exit.

B. Turbine-Internal Transfer Functions

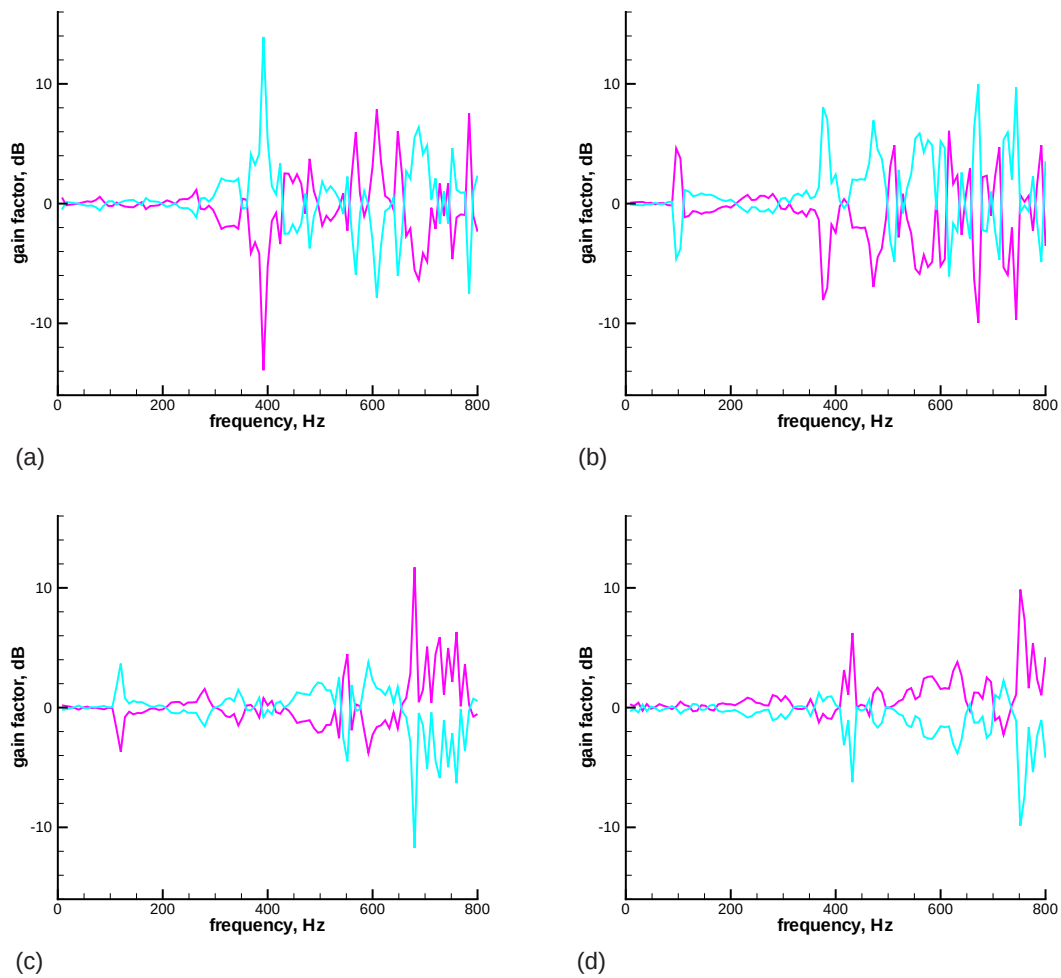

Figure 5. Narrow-band (8 Hz) turbine-internal gain factors; magenta curves—$|H_{vw}|$; cyan curves—$|H_{wv}|$; (a): 48 % corrected fan speed (flight idle); (b): 60 % corrected fan speed (approach); (c): 71 % corrected fan speed (cutback); (d): 87 % corrected fan speed (takeoff)

Figures 5 and 6 show the turbine-internal response functions determined using Eqs. (6c) and (6d), both with $\delta = 0$. Figure 5 shows the gain factor and Fig. 6 shows the phase factor, both for the four engine power settings above in panels (a)–(d). The magenta and cyan curves correspond to H_{vw} and H_{wv} results, respectively. These figures indicate that the unsteady pressure field at the turbine exit is dominated by plane waves up to about 350 Hz. Furthermore, a circumferential array with many more pressure sensors, than used in this particular configuration, would be needed to determine the azimuthal structure of the pressure field for higher frequencies.

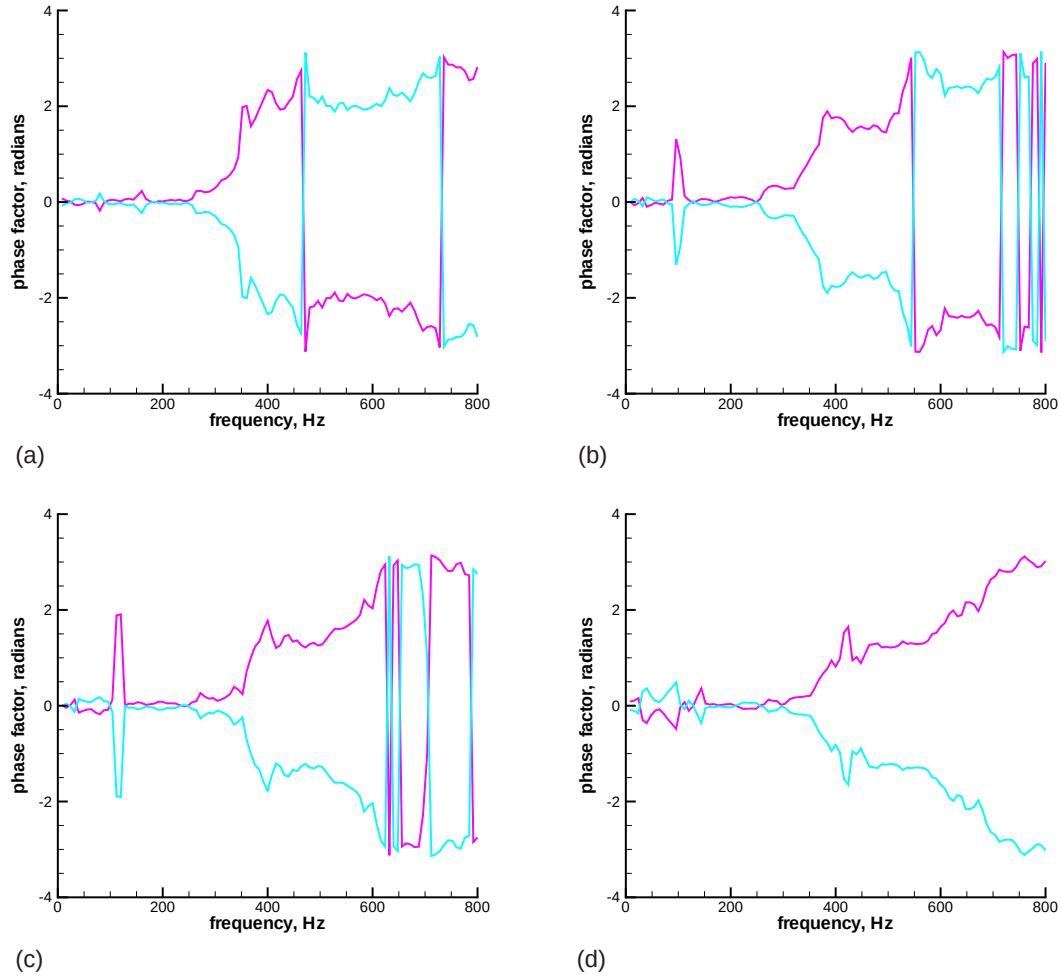

Figure 6. Narrow-band (8 Hz) turbine-internal phase factors; magenta curves—$\arg(H_{vw})$; cyan curves—$\arg(H_{wv})$; (a): 48 % corrected fan speed (flight idle); (b): 60 % corrected fan speed (approach); (c): 71 % corrected fan speed (cutback); (d): 87 % corrected fan speed (takeoff)

C. Turbine Transfer Function

Figure 7 shows the turbine-transfer gain factor, determined from Eq. (6a) with $\delta = 0$. The frequency range in this figure has been limited to 400 Hz in order not to exceed by too much the frequency range where plane waves are dominant; panels (a)–(d) correspond to the flight-idle, approach, cutback, and takeoff engine-power settings; and the red and blue curves correspond to $|H_{uv}|$ and $|H_{uw}|$ results, respectively. The turbine-transfer gain factor squared, expected normally to be less than unity, is simply the acoustic transmission loss across the turbine. Two empirical turbine transmission factors are discussed in Ref. 33.

The first one is the GE-based[34] turbine-transmission-loss formula used in ANOPP[26,27]

$$|H(f)_{A/GE}|^2 = (\Delta T_{des}/T_{ref})^{-4}\,, \tag{12}$$

where T_{des} is the design-point temperature drop across the turbine and T_{ref} is the reference temperature (ambient temperature, actual or standard sea-level value). Note that the acoustic transmission loss is essentially independent of the engine operating condition. The second formula was developed by Pratt & Whitney[4,35] and can, with a further simplification,[33] be written as

$$|H(f)_{PW}|^2 = \frac{(1+\zeta)^2}{0.8\zeta}\,, \tag{13}$$

where ζ is the ratio of the characteristic impedances across the turbine, i.e. $\zeta = \rho_{te}c_{te}/\rho_{ti}c_{ti}$ with ρ and c denoting density and speed of sound, respectively, and the subscripts 'te' and 'ti' indicating turbine exit and inlet. Both

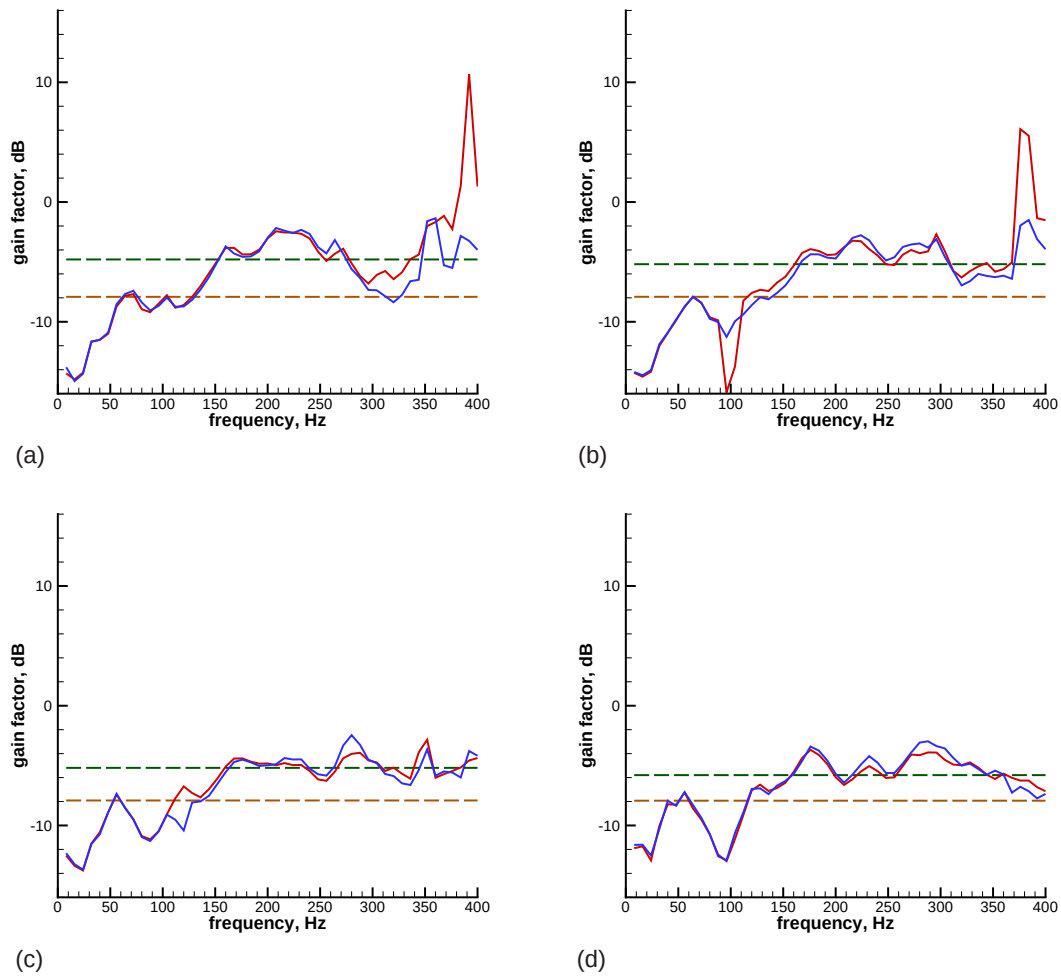

Figure 7. Narrow-band (8 Hz) turbine gain factors; red curves—$|H_{uv}|$; blue curves—$|H_{uw}|$; brown dashed line—$|H_{A/GE}|$; green dashed line—$|H_{PW}|$; (a): 48 % corrected fan speed (flight idle); (b): 60 % corrected fan speed (approach); (c): 71 % corrected fan speed (cutback); (d): 87 % corrected fan speed (takeoff)

empirical formulas, (12) and (13), are frequency independent and the corresponding gain factors are shown in Fig. 7 as brown and green dashed lines, respectively. In particular for frequencies larger than about 150 Hz, the Pratt & Whitney gain factor (13) appears to be a better fit with experimental data than the ANOPP implementation (12). From a practical point of view, this frequency range is more important than the lower-frequency range ($< 150\,Hz$) since it is expected to contain frequencies near or at the combustion noise peak.

Figure 8 shows the far-field results in the 130° direction of the three source-separation procedures carried out by Hultgren and Miles,[25] on the same EVNERT dataset as here, as well as the effects on their ANOPP predictions by replacing the ANOPP turbine-attenuation factor by the simplified Pratt & Whitney formula. The 1/3-octave sound-pressure-level (SPL) results are shown at the four engine power settings of 48, 60, 71, and 87 percent corrected fan speed (flight-idle, approach, cutback, and takeoff conditions) for the 1/3-octave center frequency range of 20 to 1000 Hz. The solid lines represent the original ANOPP 1/3-octave SPL predictions for the total (dark-gray) and combustion (red-brown) noise. The symbols correspond to results computed from the experimental time histories as described in Ref. 25. The black squares, labeled G_{zz}, represent the total noise signature, which is reasonably well predicted by the original ANOPP results. The gray squares, labeled NOP, correspond to the threshold value for the coherent output power and any combustion-noise result below these values would not be meaningful using the number of data segments and source-separation techniques used in their work. The blue, red, and green squares correspond to the combustion noise detected using the three methods labeled ‘2s-cip1’, ‘2s-t551’, and ‘3s’, respectively (see Ref. 25 for details). The dashed curves represent the present post-corrected ANOPP 1/3-octave SPL predictions for the total (dark-gray) and combustion (red-brown) noise using the Pratt & Whitney acoustic turbine-transmission formula (13)

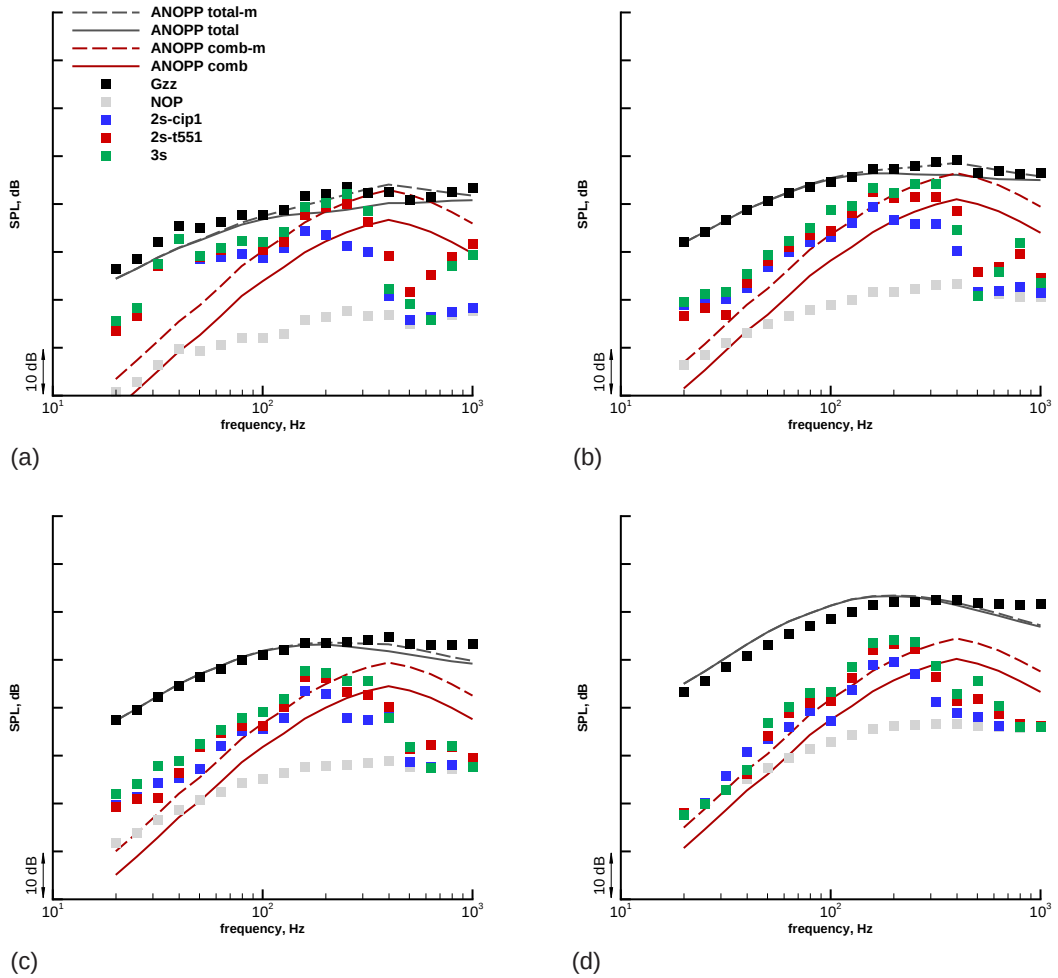

Figure 8. Total and combustion noise 1/3-octave SPL versus 1/3-octave center frequency in the 130° direction; symbols and solid lines—data and ANOPP predictions from Ref. 25; dashed lines—ANOPP predictions modified to use the P&W turbine-attenuation; (a): 48 % corrected fan speed (flight idle); (b): 60 % corrected fan speed (approach); (c): 71 % corrected fan speed (cutback); (d): 87 % corrected fan speed (takeoff)

rather than the one build into ANOPP (12). It is clear from panels (a)–(c) in Fig. 8 that the total noise signature is better predicted by the modified ANOPP results than the original ones. One can also argue that the combustion-noise prediction is also improved by examining the source-separated results in this figure, although the situation is not as clear for frequencies larger or equal to 400 Hz.

Figure 9 shows the turbine-transfer phase factor, determined from Eq. (6b) with $\delta = 0$. In this figure, the frequency range has been limited to 400 Hz in order to only slightly exceed the frequency range where plane waves are dominant; panels (a)–(d) correspond to the flight-idle, approach, cutback, and takeoff engine-power settings; and the red and blue curves correspond to $\arg(H_{uv})$ and $\arg(H_{uw})$ results, respectively. It can be seen that the phase changes by about 4.5 radians from 0 to 200 Hz. This indicates that in this frequency range there is a signal time delay of about 3.6 ms, which strongly implies[5,6] that the combustion noise is dominated by indirect noise.

Figure 10 shows the ratio of the actual transfer function and the directly measurable transfer function. It clearly indicates the error caused by the noise-to-signal ratio at the combustor location if H_{xy} and H_{xz} are used as approximations for the actual combustion-noise transfer functions H_{uv} and H_{uw}.

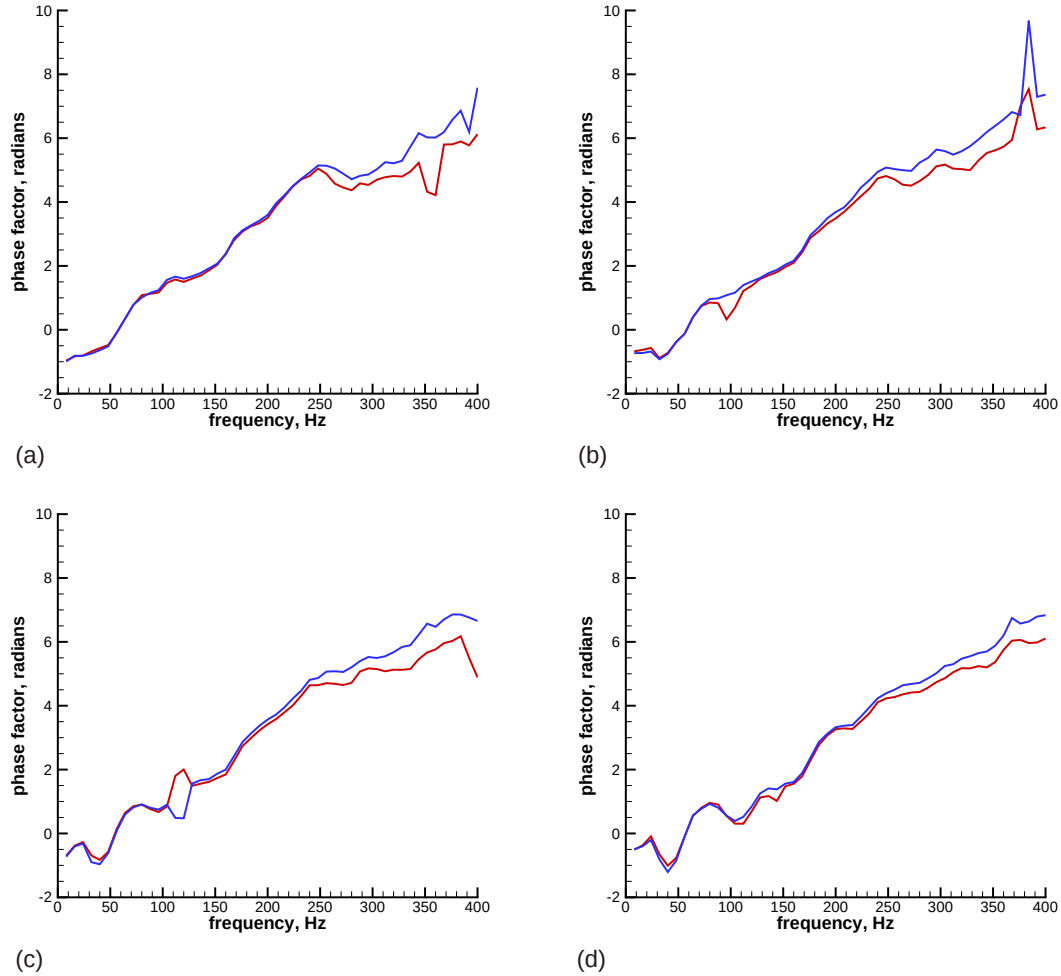

Figure 9. Narrow-band (8 Hz) turbine phase factors; red curves—$\arg(H_{uv})$; blue curves—$\arg(H_{uw})$; (a): 48 % corrected fan speed (flight idle); (b): 60 % corrected fan speed (approach); (c): 71 % corrected fan speed (cutback); (d): 87 % corrected fan speed (takeoff)

IV. Summary and Conclusions

NASA/Honeywell EVNERT[28] full-scale static engine test data has been analyzed by using source-separation techniques in order to determine the turbine transfer of combustor noise. The true combustion-noise turbine-transfer function was educed from the data by using a three-signal approach. The resulting gain factors were compared with the corresponding constant values obtained from ANOPP/GE and Pratt & Whitney empirical acoustic-turbine-loss formulas. It was found that the Pratt & Whitney formula agrees better with the experimental results for frequencies of practical importance.

The far-field 1/3-octave SPL results in the 130° direction of Hultgren and Miles[25] were reexamined using a post-correction of their ANOPP predictions for both the total noise signature and the combustion-noise component. It was found that replacing the standard ANOPP turbine-attenuation function for combustion noise with the Pratt & Whitney one clearly improved the total-noise predictions and also improved the combustion-noise predictions. The latter comparison was not as conclusive as the former due to the inherent difficulty in extracting the combustion-noise component from the total noise signature. However, the former would not be true if the combustion-noise component predictions had not been improved by the attenuation-formula change.

Based on these results, it is recommended that *the GECOR combustion-noise module in ANOPP be updated to allow for a user-selectable switch between the current transmission-loss model (12) and the simplified Pratt & Whitney formula (13).*

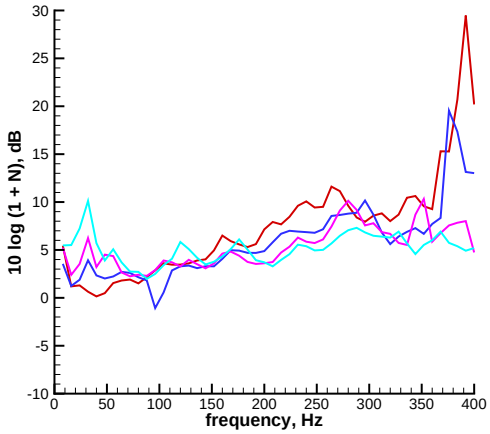

Figure 10. Narrow-band (8 Hz) combustor-noise factor $1 + N_u(f)$; red curve: 48 % corrected fan speed (flight idle); blue curve: 60 % corrected fan speed (approach); magenta curve: 71 % corrected fan speed (cutback); cyan curve: 87 % corrected fan speed (takeoff)

References

[1]Cumpsty, N. A. and Marble, F. E., "The Interaction of Entropy Fluctuations with Turbine Blade Rows; a Mechanism of Turbojet Engine Noise," *Proc. R. Soc. Lond. A*, Vol. 357, 1977, pp. 323–344.

[2]Cumpsty, N. A. and Marble, F. E., "Core Noise from Gas Turbine Exhausts," *J. Sound and Vibration*, Vol. 54, No. 2, 1977, pp. 297–309.

[3]Cumpsty, N. A., "Jet Engine Combustion Noise: Pressure, Entropy and Vorticity Perturbations Produced by Unsteady Combustion or Heat Addition," *J. Sound and Vibration*, Vol. 66, No. 4, 1979, pp. 527–544.

[4]Mathews, D. C., Rekos, Jr, N. F., and Nagel, R. T., "Combustion Noise Investigation," Tech. Rep. FAA RD-77-3, FAA, 1977.

[5]Miles, J. H., "Spectral Separation of the Turbofan Engine Coherent Combustion Noise Component," Tech. Rep. AIAA Paper 2008-0050 (NASA TM-2008-215157), 46th Aerospace Sciences Meeting, Reno, Nevada, 2008.

[6]Miles, J. H., "Time Delay Analysis of Turbofan Engine Direct and Indirect Combustion Noise Sources," *J. Propulsion and Power*, Vol. 25, No. 1, 2009, pp. 218–227.

[7]Bendat, J. S. and Piersol, A. G., *Engineering Applications of Correlation and Spectral Analysis*, Wiley-Interscience, 1980.

[8]Karchmer, A. M. and Reshotko, M., "Core Noise Source Diagnostics on a Turbofan Engine Using Correlation and Coherence Techniques," Tech. Rep. NASA TM-X-73535, NASA, 1976.

[9]Reshotko, M., Karchmer, A. M., Penko, P. F., and McArdle, J. G., "Core Noise Measurements on a YF-102 Turbofan Engine," *J. Aircraft*, Vol. 14, No. 7, 1977, pp. 611–612.

[10]Karchmer, A. M., "Identification and Measurement of Combustion Noise from a Turbofan Engine Using Correlation and Coherence Techniques," Tech. Rep. NASA TM-73747, NASA, 1977.

[11]Karchmer, A. M., Reshotko, M., and Montegani, F. J., "Measurement of Far-Field Combustion Noise from a Turbofan Engine Using Coherence Functions," Tech. Rep. AIAA Paper 1977-1277 (NASA TM-73748), 4th AIAA Aeroacoustics Conference, Atlanta, Georgia, 1977.

[12]Chung, J. Y., "Rejection of Flow Noise Using a Coherence Function Method," *J. Acoustical Society of America*, Vol. 62, No. 2, 1977, pp. 388–395.

[13]Reshotko, M. and Karchmer, A. M., "Core Noise Measurements from a Small, General Aviation Turbofan Engine," Tech. Rep. NASA TM-81610, NASA, 1980.

[14]Doyle, V. L. and Moore, M. T., "Core Noise Investigation of the CF6-50 Turbofan Engine," Tech. Rep. NASA CR-159749, NASA, 1980.

[15]Krejsa, E. A., "New Technique for the Direct Measurement of Core Noise from Aircraft Engines," Tech. Rep. AIAA Paper 1981-1587 (NASA TM-82634), 17th AIAA/SAE/ASME Joint Propulsion Conference, Colorado Springs, Colorado, 1981.

[16]Krejsa, E. A., "Application of 3-Signal Coherence to Core Noise Transmission," Tech. Rep. AIAA Paper 1983-0759 (NASA TM-83333), 8th AIAA Aeroacoustics Conference, Atlanta, Georgia, 1983.

[17]Shivashankara, B. N., "High Bypass Ratio Engine Noise Component Separation by Coherence Technique," *J. Aircraft*, Vol. 20, No. 3, 1983, pp. 236–242.

[18]Krejsa, E. A., "Combustion Noise From Gas Turbine Aircraft Engines Measurement of Far-Field Levels," Tech. Rep. NASA TM-88971, NASA, 1987.

[19]Hsu, J. S. and Ahuja, K. K., "A Coherence-Based Technique to Separate Internal Mixing Noise From Farfield Measurements," Tech. Rep. AIAA Paper 1998-2296, 4th AIAA/CEAS Aeroacoustic Conference, Toulouse, France, 1998.

[20]Karchmer, A. M., "Acoustic Modal Analysis of a Full Scale Annular Combustor," Tech. Rep. AIAA Paper 1983-0760 (NASA TM-83334), 8th AIAA Aeroacoustics Conference, Atlanta, Georgia, 1983.

[21]Miles, J. H. and Krejsa, E. A., "Pressure Transfer Function of a JT15D Nozzle due to Acoustic and Convected Entropy Fluctuations," *J. Acoustical Society of America*, Vol. 72, No. 6, 1982, pp. 2008–2019.

[22]Krejsa, E. A. and Karchmer, A. M., "Acoustic Modal Analysis of the Pressure Field in the Tailpipe of a Turbofan Engine," Tech. Rep. NASA TM-83387, NASA, 1983.

[23]Miles, J. H., Wasserbauer, C. A., and Krejsa, E. A., "Cross Spectra Between Temperature and Pressure in a Constant Area Duct Downstream of a Combustor," Tech. Rep. AIAA Paper 1983-0762 (NASA TM-83351), 8th AIAA Aeroacoustics Conference, Atlanta, Georgia, 1983.

[24]Royalty, C. M. and Schuster, B., "Noise from a Turbofan Engine Without a Fan from the Engine Validation of Noise and Emission Reduction Technology (EVNERT) Program," Tech. Rep. AIAA 2008-2810, 14th AIAA/CEAS Aeroacoustics Conference, Vancouver, British Columbia, 2008.

[25]Hultgren, L. S. and Miles, J. H., "Noise-Source Separation Using Internal and Far-Field Sensors for a Full-Scale Turbofan Engine," Tech. Rep. AIAA Paper 2009-3220 (NASA TM-2009-215834), 15th AIAA/CEAS Aeroacoustic Conference, Miami, Florida, 2009.

[26]Zorumski, W. E., "Aircraft Noise Prediction Program Theoretical Manual, Part 1," Tech. Rep. NASA TM-83199-Pt-1, NASA, 1982.

[27]Zorumski, W. E., "Aircraft Noise Prediction Program Theoretical Manual, Part 2," Tech. Rep. NASA TM-83199-Pt-2, NASA, 1982.

[28]Weir, editor, D. S., "Engine Validation of Noise and Emission Reduction Technology Phase I," Tech. Rep. NASA CR-2008-215225, NASA, 2008, Honeywell Report No. 21-13843, Honeywell Aerospace, Phoenix, Arizona.

[29]Mendoza, J. M., Nance, D. K., and Ahuja, K. K., "Source Separation from Multiple Microphone Measurements in the Far Field of a Full Scale Aero Engine," Tech. Rep. AIAA Paper 2008-2809, 14th AIAA/CEAS Aeroacoustic Conference, Vancouver, British Columbia, 2008.

[30]Brillinger, D. R., *Time Series Data Analysis and Theory*, Holden-Day, 1981.

[31]Miles, J. H., "Aligned and Unaligned Coherence: A New Diagnostic Tool," Tech. Rep. AIAA Paper 2006-0010 (NASA TM-2006-214112), 44th Aerospace Sciences Meeting, Reno, Nevada, 2006.

[32]Welch, P. D., "The Use of Fast Fourier Transform for the Estimation of Power Spectra: A Method Based on Time Averaging Over Short, Modified Periodograms," *IEEE Transactions on Audio and Electroacoustics*, Vol. AU-15, No. 2, 1967, pp. 70–73.

[33]Mahan, R. J. and Karchmer, A., "Combustion and Core Noise," *Aeroacoustics of Fligh Vehicles: Theory and Practice*, edited by H. H. Hubbard, Vol. 1, chap. 9, NASA Reference Publication 1258, WRDC Technical Report 90-3052, 1991, pp. 483–517.

[34]Motsinger, R., "Prediction of Engine Combustor Noise and Correlation with T64 Engine Low Frequency Noise," Tech. Rep. R72AEG313, General Electric Co., 1972.

[35]Mathews, D. C. and Rekos, Jr, N. F., "Prediction and Measurement of Direct Combustion Noise in Turbopropulsion Systems," *J. Aircraft*, Vol. 14, No. 9, 1977, pp. 850–859.

REPORT DOCUMENTATION PAGE	Form Approved OMB No. 0704-0188

The public reporting burden for this collection of information is estimated to average 1 hour per response, including the time for reviewing instructions, searching existing data sources, gathering and maintaining the data needed, and completing and reviewing the collection of information. Send comments regarding this burden estimate or any other aspect of this collection of information, including suggestions for reducing this burden, to Department of Defense, Washington Headquarters Services, Directorate for Information Operations and Reports (0704-0188), 1215 Jefferson Davis Highway, Suite 1204, Arlington, VA 22202-4302. Respondents should be aware that notwithstanding any other provision of law, no person shall be subject to any penalty for failing to comply with a collection of information if it does not display a currently valid OMB control number.
PLEASE DO NOT RETURN YOUR FORM TO THE ABOVE ADDRESS.

1. REPORT DATE *(DD-MM-YYYY)*	2. REPORT TYPE	3. DATES COVERED *(From - To)*
01-02-2012	Technical Memorandum	

4. TITLE AND SUBTITLE	5a. CONTRACT NUMBER
Full-Scale Turbofan-Engine Turbine-Transfer Function Determination Using Three Internal Sensors	5b. GRANT NUMBER
	5c. PROGRAM ELEMENT NUMBER
6. AUTHOR(S) Hultgren, Lennart, S.	5d. PROJECT NUMBER
	5e. TASK NUMBER
	5f. WORK UNIT NUMBER WBS 561581.02.08.03.18.13
7. PERFORMING ORGANIZATION NAME(S) AND ADDRESS(ES) National Aeronautics and Space Administration John H. Glenn Research Center at Lewis Field Cleveland, Ohio 44135-3191	8. PERFORMING ORGANIZATION REPORT NUMBER E-18007
9. SPONSORING/MONITORING AGENCY NAME(S) AND ADDRESS(ES) National Aeronautics and Space Administration Washington, DC 20546-0001	10. SPONSORING/MONITOR'S ACRONYM(S) NASA
	11. SPONSORING/MONITORING REPORT NUMBER NASA/TM-2012-217252

12. DISTRIBUTION/AVAILABILITY STATEMENT
Unclassified-Unlimited
Subject Category: 71
Available electronically at http://www.sti.nasa.gov
This publication is available from the NASA Center for AeroSpace Information, 443-757-5802

13. SUPPLEMENTARY NOTES

14. ABSTRACT
Noise-source separation techniques, using three engine-internal sensors, are applied to existing static-engine test data to determine the turbine transfer function for the currently subdominant combustion noise. The results are used to assess the combustion-noise prediction capability of the Aircraft Noise Prediction Program (ANOPP) and an improvement to the combustion-noise module GECOR is suggested. The work was carried out in response to the NASA Fundamental Aeronautics Subsonic Fixed Wing Program's Reduced-Perceived-Noise Technical Challenge.

15. SUBJECT TERMS
Turbofan engine; Function transfer; Internal sensors

16. SECURITY CLASSIFICATION OF:			17. LIMITATION OF ABSTRACT	18. NUMBER OF PAGES	19a. NAME OF RESPONSIBLE PERSON
a. REPORT	b. ABSTRACT	c. THIS PAGE			STI Help Desk (email:help@sti.nasa.gov)
U	U	U	UU	20	19b. TELEPHONE NUMBER *(include area code)* 443-757-5802